Performance of Dual-Bridge High Frequency Resonant DC/DC Converter for Energy Storage Application

Gurupal K. Gaidhane[1]
PG Research Scholar, Department of Electrical Engineering
Government College of Engineering
Amravati, India.
gurupal.gaidhane@gmail.com

A. S. Sindekar[2]
Head, Department of Electrical Engineering
Government College of Engineering
Amravati, India.
assindekar@rediffmail.com

***Abstract*—A bidirectional dual-bridge high-frequency isolated resonant DC-DC converter is gaining more attention in renewable energy system due to its high power density, small size, reducing stress and removing electromagnetic interference noise. In this paper the simulation of dual bridge LC-L resonant converter is carried out in Simulink for resistive and battery load. The simplified steady state analysis using complex ac analysis is given and conditions for zero voltage switching are presented accordingly. A closed loop control operation of a converter using PI controller is suggested to minimize the reverse power flow for battery load.**

Keywords—DC-DC converter, dual active bridge (DAB), renewable energy sources, zero -voltage switching (ZVS).

I. INTRODUCTION

With the increasing demand for electric power in future automobiles, telecom and computer system, hybrid vehicle system and aviation system, people have recognized the key importance of renewable energy sources to these systems [1]-[3]. The bidirectional dc-dc converter plays an important role to interface between high voltage bus where energy generation device such as photovoltaic panel or other sources are installed, and a low voltage bus, where generally energy storage devices such as a battery or super capacitor is connected [4] as shown in fig. 1. The input to this converter is generally variable dc voltage sources like fuel cell, photovoltaic or ac sources with both changing in magnitude and frequency. The output of this converter is dc which can be fed to dc load, energy storage device or fed to utility through an inverter. The power level of such type of converter is generally less than 100 kW [5]. A dual bridge converter (DBC) is generally consisting of two active bridges linked by high frequency transformer and power transfer inductor. The operating frequency of DBC is very high which offers many advantages like smaller size and light weight of reactive components, power supply with faster transient response [6]. Compared to traditional dc-dc converter, the bidirectional dual active bridge (DAB) have many advantages, like electrical isolation, high reliability ease of soft switching control and bidirectional power flow.

Various topologies variations for DC-DC converters of high power applications with bidirectional power transfer have been proposed and developed through the last four decades. For the development of the efficient power, dc-dc converter they use either resonant [7], soft switch achieved by controlling phase shift [8]-[9], or hard pulse width modulation

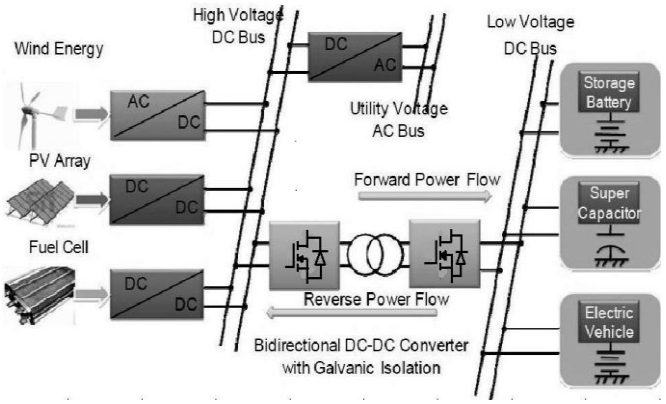

Fig. 1. Typical application of isolated bidirectional dc-dc converter for power distribution in a microgrid.

(PWM) [9]. Even though PWM and soft switched achieved by controlling phase shift converters have their own advantages but, they have also limitations to use for middle power bidirectional dc-dc converters. These converter topologies aren't efficient to use for middle bidirectional dc-dc converters due to the following drawbacks;

- large number of switches
- large components
- limited range of satisfactory for high frequency
- Complex power and control circuit etc.

As high power applications, medium and low power bidirectional dc-dc converters are based on hard switching [10], soft switching or resonant switching type [11]. Most of these dc-dc converters are well suited for a particular application even though they have their own drawback. Their limitations can be described as;

- lack of isolation
- high component stresses
- large ripple current through the filtering inductors
- At high frequencies the converter designed to operate under resonance and soft switching may suffer from hard switching of the devices.

The dual active bridge resonant converter is a combination of two active bridges with resonant tank as shown in fig. 2. Two active bridges are linked by a high frequency (HF) transformer and resonant tank. The resonant tank is either series resonant or parallel resonant or combination of both. It can be capacitor, inductor, series combination of LC or parallel

combination of

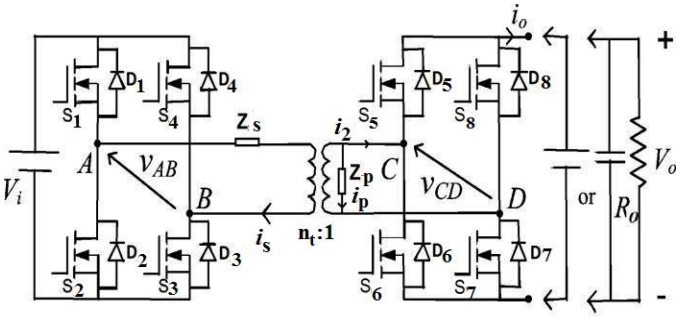

Fig. 2. A dual-bridge converter with a generalized resonant tank

LC. Z_p is an impedance of parallel resonant tank which can be put on any side of transformer. The series resonant converter has drawback of voltage regulation at light load while parallel resonant converter cause low efficiency at reduced load due to circulating current. Series-parallel LC-L resonant converters overcome most of the limitations of series and parallel resonant converters. The magnetizing and leakage inductance of a HF transformer could be utilized as part of series resonant tank Z_s and parallel resonant tank Z_p respectively [8]. The power flow through the resonant tank can be controlled by controlling phase shift between the gating signals of the two bridges.

In this paper the approximate analysis using complex circuit analysis method is used to analyze the converter and conditions for ZVS is derived accordingly. Simulation results for both resistive and battery load are included for the purpose of validation. A suitable closed-loop control strategy has been used for battery load to minimize the reverse power flow.

II. Modified Complex AC Analysis Approach for Dual-Bridge High Frequency Resonant DC/DC Converter

In complex ac analysis approach, only fundamental component of voltages and currents are considered while all other harmonics are neglected. It is assumed that all switches, diodes and transformer are ideal [7] [10]. The leakage and magnetizing part of transformer are used as a part of series and parallel resonant tank by proper arrangement. The effect of snubber circuit is also neglected. All the parameters on secondary side of HF transformer have been taken to primary side and are denoted by superscript " ' ". The reactances of Z_P and Z_S are defined as X_P and X_S respectively. Two ac equivalent circuit analysis methods are given for dc voltage source load and resistive load with capacitive filter, respectively. Both methods could be applied for either of the two types of load (*ie.* Battery or resistive load), because the load resistance can be regarded as the equivalent load resistance of a dc voltage source with the designed power at $P_o = V_o^2/R_F$, where R_F is full load resistance. The equivalent circuit of converter in phasor domain can be drawn as shown in fig. 3.

For convenience the base values are taken as bellow:

$$V_B = V_1; Z_B = R'_F; I_B = V_B / Z_B \quad (1)$$

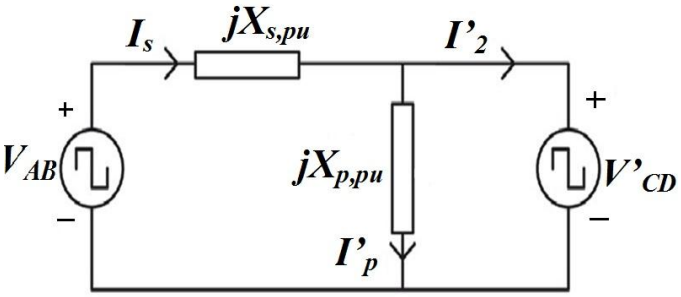

Fig. 3. The equivalent circuit of the dual-bridge resonant converter with generalized resonant tank.

Where, R'_F is the primary side reflected equivalent full load resistance, which is given as:

$$R'_F = {n_t}^2 * ({V_0}^2/P_0) \quad (2)$$

The normalized frequency *F* is given by:

$$F = \omega_s/\omega_r = f_s/f_r \quad (3)$$

Where $f_s = \omega_s/2\pi$ is switching frequency and $f_r = \omega_r/2\pi = 1/2\pi\sqrt{L_s C_s}$ is frequency of a resonant tank. The normalized values of all the reactances are given by:

$$X_{s,pu} = X_s/Z_B \quad (4)$$

$$X_{p,pu} = X'_p/Z_B \quad (5)$$

Where X_s is a reactance of series resonant tank and $X'_p = n_t^2 X_p$ is a primary side reflected reactance of parallel resonant tank.

Since output voltage of secondary side converter V'_o is assumed to be constant, the reflected converter input voltage V'_{CD} is a square wave with magnitude of V'_o. Thus the *rms* value of fundamental input voltage V'_{CD} is given as:

$$V'_{CD,rms} = \frac{4}{\sqrt{2}\pi} V'_o \quad (6)$$

The secondary bridge input current i'_2 is assumed to be approximately sinusoidal. Due to active rectifier control, the rectifier input current i'_2 is assumed to lead the voltage V'_{CD} by phase shift angle $-\theta$. Thus *rms* value of secondary current is given by:

$$I'_{2\,rms} = \frac{\pi}{\sqrt{8}\cos\theta} I'_o \quad (6)$$

Where I'_o is an average value of i'_o.

Because of active rectifier, output current i'_o may go negative for small portion of each cycle, which means sometimes power is transferred form secondary side to

primary side. Thus in case of conventional complex ac analysis it is pertinent to represent the whole secondary part with an equivalent impedance $Z_{ac} = Z_{ac} \angle -\theta$ instead of pure resistance

The magnitude of equivalent ac impedance is obtained from equations (5) and (6).

$$Z_{ac} = \frac{V'_{XY\,rms}}{I'_{2\,rms}} = \frac{8V'_2 \cos\theta}{\pi^2 I'_o} = \frac{8\,R'_o \cos\theta}{\pi^2} \quad (7)$$

The normalize ac impedance is given as:

$$Z_{ac,pu} = \frac{Z_{ac}}{R'_F} = \frac{8\,R'_o \cos\theta}{\pi^2\,R'_F} = \frac{8\,\cos\theta}{\pi^2} H \quad (8)$$

Where $R_o{}'$ is a output load resistance while $H=R_o{}'/R'_F$ is normalized load resistance and H $\in [1, \infty]$ as load goes on decreasing from full load to zero load.

With equivalent impedance, the converter equivalent circuit in phasor domain can be drawn as shown in fig. 4.

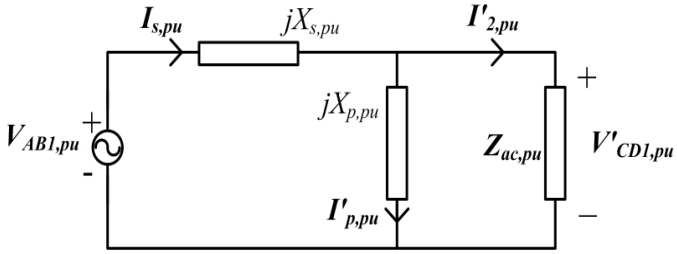

Fig. 4. The phasor domain equivalent circuit of the dual-bridge resonant converter with equivalent impedance.

$V_{AB1,\,pu}$ and $V'_{CD1,pu}$ are the normalized fundamental phasor components of V_{AB} and V'_{CD} respectively. The expressions for normalized fundamental components of V_{AB} and V'_{CD} in phasor domain are:

$$V_{AB1,\,pu} = \frac{4}{\pi} e^{j(\omega_s t - \frac{\pi}{2})} \quad (9)$$

$$V'_{CD1,pu} = \frac{4\,M}{\pi} e^{\left(\omega_s t - \emptyset - \frac{\pi}{2}\right)} \quad (10)$$

Here $\emptyset$ is phase angle between primary side voltage $V_{AB1,\,pu}$ and secondary side voltage $V'_{CD1,pu}$ which obtained by providing delay in gating signals of secondary converter with respect to gating signals of primary converter. *M* is the converter gain, given as:

$$M = \frac{V'_0}{V_i} \quad (11)$$

By using principle of superposition, the three current phasors can be evaluated as:

$$I_{s,pu}(t) = \frac{4}{\pi X_{s,pu}} \left(M e^{-j\emptyset} - 1\right) e^{j\omega_s t} \quad (12)$$

$$I'_{2,pu}(t) = \frac{4}{\pi X_{s,pu}} [M(1+K) e^{-j\emptyset} - 1)] e^{j\omega_s t} \quad (13)$$

$$I'_{p,pu}(t) = -\frac{4M}{\pi X_{p,pu}} e^{j(\omega_s t - \emptyset)} \quad (14)$$

where:

$$K = \frac{\omega_s L_s - (1/\omega_s C_s)}{\omega_s L_p} = \frac{L_s}{L_p} \left(1 - \frac{1}{F^2}\right) \quad (15)$$

Thus the resonant currents in time domain can be obtained as:

$$i_{s,pu}(t) = \frac{4[M\cos(\omega_s t - \emptyset) - \cos(\omega_s t)]}{\pi X_{s,pu}} \quad (16)$$

$$i'_{2s,pu}(t) = \frac{4[M\cos(\omega_s t - \emptyset)(1+K) - \cos(\omega_s t)]}{\pi X_{s,pu}} \quad (17)$$

. $$i_{p,pu}(t) = -\frac{4M\cos(\omega_s t - \emptyset)}{\pi X_{p,pu}} \quad (18)$$

The soft switching conditions for two bridges are [7]:

$i_{s,pu}(0)$ < 0 for the primary bridge, and (19)

$i'_{2s,pu}\left(\frac{\emptyset}{\omega_s}\right)$ > 0 for the secondary bridge. (20)

With the help of equations (16) and (17) the conditions can be re-written as:

$$\frac{4[M\cos(\emptyset) - 1]}{\pi X_{s,pu}} < 0 \quad (21)$$

$$\frac{4[M(1+K) - \cos(\emptyset)]}{\pi X_{s,pu}} > 0 \quad (22)$$

The solution to realize zero voltage switching of two bridges is:

$$\cos\emptyset < \min\left\{\frac{1}{M},\, M(1+K)\right\} \quad (23)$$

To satisfy equation (23) it is better that both *1/M* and *M (1+K)* are greater than 1 because maximum value of cos $\emptyset$ is 1. For this *M* should be less than one so that the soft switching of primary bridge is possible and once $M \leq 1$ soft switching of secondary bridge is possible by properly selecting the value of *K*.

The switch peak currents on both side of HF transformer are:

$$I_{s,pu} = \frac{4\sqrt{M^2 + 1 - 2M\cos\emptyset}}{\pi\,|X_{s,pu}|} \quad (24)$$

$$I'_{2p,pu} = \frac{4\sqrt{(M+MK)^2 + 1 - 2M(1+K)\cos\emptyset}}{\pi |X_{s,pu}|} \quad (25)$$

The converter gain *M* can also be given from fig. 4 as:

$$M = \left| \frac{Z_{ac,pu} \parallel jX_{p,pu}}{X_{s,pu} + Z_{ac,pu} \parallel jX_{p,pu}} \right| = f(\theta) \quad (26)$$

From equation (26) it is concluded that *M* is a function of θ, which is difference of angle between $V_{CD1,\,pu}$ and $I'_{2,pu}$. Here θ is not a controllable parameter; hence *M* can be controlled by controlling another angle β, which is a difference between $V_{AB1,\,pu}$ and $I'_{2,pu}$, given as:

$$\theta = \emptyset - \beta \quad (27)$$

Where,

$$\beta = -tan^{-}\left(\frac{(1+K) Z_{ac,pu} \sin\theta}{(1+K) Z_{ac,pu} \cos\theta - X_{s,pu}} \right) \quad (28)$$

Hence from equations (26), (27) and (28) *M* can be expressed as:

$$M = \frac{8\, H \sin\emptyset}{\pi^2\, X_{s,pu}} \quad (29)$$

From equation (29) it is concluded that *M* is a function of $\emptyset$, therefore *M* can be adjusted by taking appropriate value of $\emptyset$.

III. Simulation Results

The simulation of dual-bridge LC-L resonant converter is carried out in Simulink software for both resistive and battery load, and the analysis is done accordingly.

A. Simulation results for resistive load

The dual-bridge LC-L converter is assumed to work at the following conditions:

V_1 = 200V, V_o = 48V, M = 0.9761, F = 1.09, K =0.3, f_s = 100 kHz.

$J = I_0/n_t I_B$=0.25 (30)

The resonant tank components can be taken as

$$L_s = \frac{{v_i}^2\, MJF}{P_o \omega_s} = 87.54\mu H \quad (31)$$

$$C_s = \frac{P_o F}{{V_i}^2 MJ \omega_s} = 35nF \quad (32)$$

$$L'_p = 875.4\mu H \quad (33)$$

$$L_p = {L'_p}\Big/{n_t}^2 = 50.42\mu H \quad (34)$$

The capacitive filter connected at output side is given by:

$$C = \frac{1}{4\sqrt{3}\, f_s\, \gamma\, R_L} \quad (35)$$

The full load (200 W) and half load (100 W) operations are presented in fig. 5 and fig. 6 respectively. The ZVS operation is confirmed from the current vs. time plot of switches. The output current of secondary bridge is i_o, whose average value is output dc current. The negative part of i_o present only for small portion of each cycle which indicates low circulating current and high efficiency. The current in parallel inductor which is placed on secondary side of HF transformer, only relies on output voltage and is independent on load level. Comparison between Simulated and calculated values of various parameters is given in following Table.

TABLE I
COMPARISION BETWEEN SIMULATED AND CALCULATED VALUES OF PARAMETERS AT *V_i = 200V, V_O = 48V AND f_S=100kHz.*

Load Level	Parameters	Simulated value	Calculated value
Full Load 200W	M	0.9761	0.9792
	I_s	1.64A	1.45A
	I_2	6A	7.5A
	$\emptyset$	3.6°	3.3°
Half Load 100W	M	0.9792	0.95
	I_s	0.84A	0.76A
	I_2	3.2A	3.16A
	$\emptyset$	1.8°	1.6°

B. Simulation results for battery load

The simulation of LCL resonant converter is performed in Simulink for different battery charging conditions. The ZVS is conformed from simulation plots of fig. 7. While performing simulations for battery load it is observed that as the battery charging goes on increasing the amount of reverse power flow from battery side to source increases i.e. negative part of i_o goes on increasing. This leads to reduce the efficiency of converter and high conversion losses which results in slow rate of battery charging. Here simulation results of LC-L converter for battery load at 90% of state of charging (SOC) are presented.

The converter works at following conditions:
V_1=200V; V_2=50V; Battery =1.52Ah. 48V, $\emptyset$ =1.5°

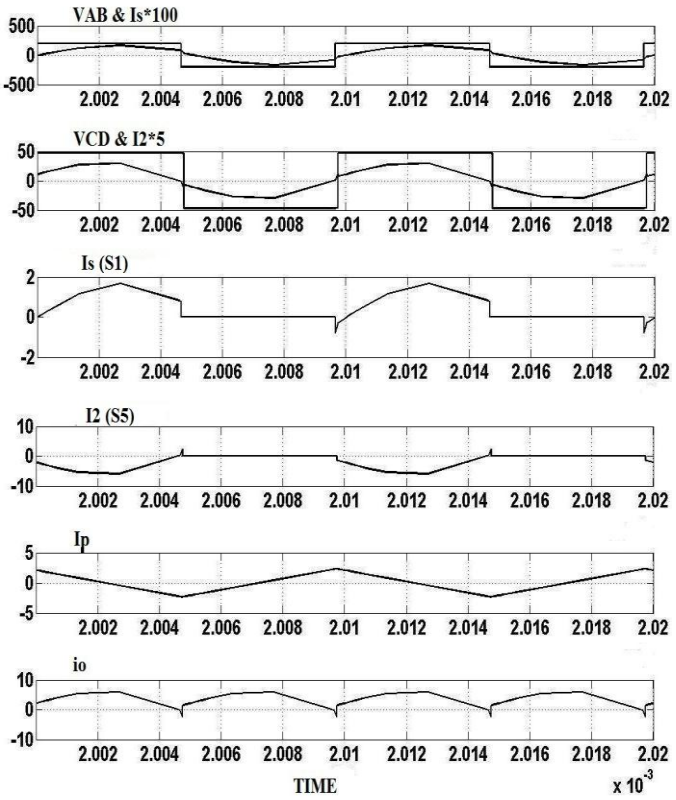

Fig. 5. Simulation results of a dual-bridge LC-L resonant converter at $P_o = 200\ W$, $V_o = 48\ V$ for resistive load

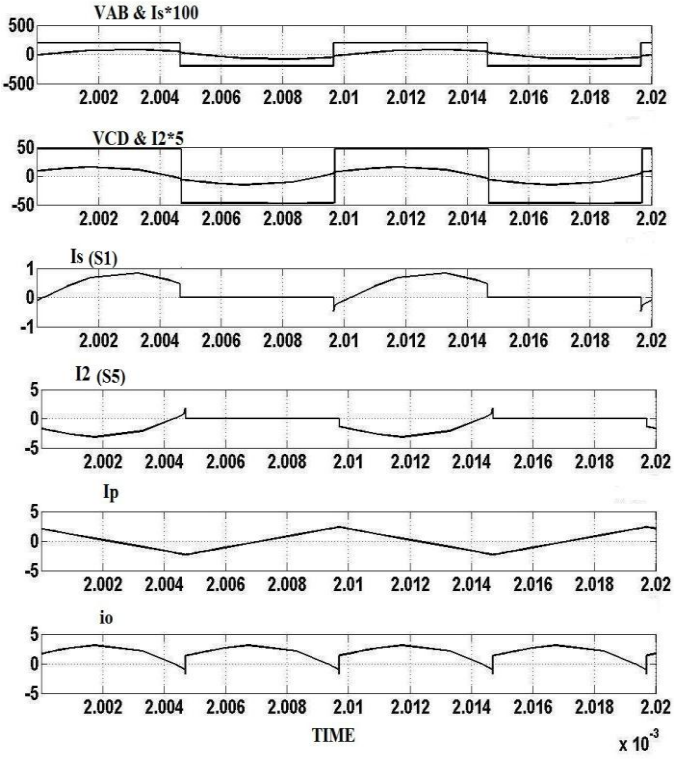

Fig. 6. Simulation results of a dual-bridge LC-L resonant converter at $P_o = 100\ W$, $V_o = 48\ V$ for resistive load

From fig. 7 it is observed that as reverse power flow from load side (battery side) to source side is more which leads to increase in power loss of a converter, thus there is necessity to design a suitable controller to prevent the reverse power flow and minimize the power loss. Comparison between Simulated and calculated values of various parameters is given in following Table.

TABLE 2.

COMPARISON BETWEEN SIMULATED AND CALCULATED VALUES OF PARAMETERS AT $V_i = 200V$, $V_O = 50V$ AND $f_S = 100kHz$.

SOC	Parameters	Simulated	Calculated
90% ≈35ohm	M	0.98	0.95
	I_s	0.36A	0.5A
	I_2	2.5A	2.5A
	∅	1.8^o	1.5^o

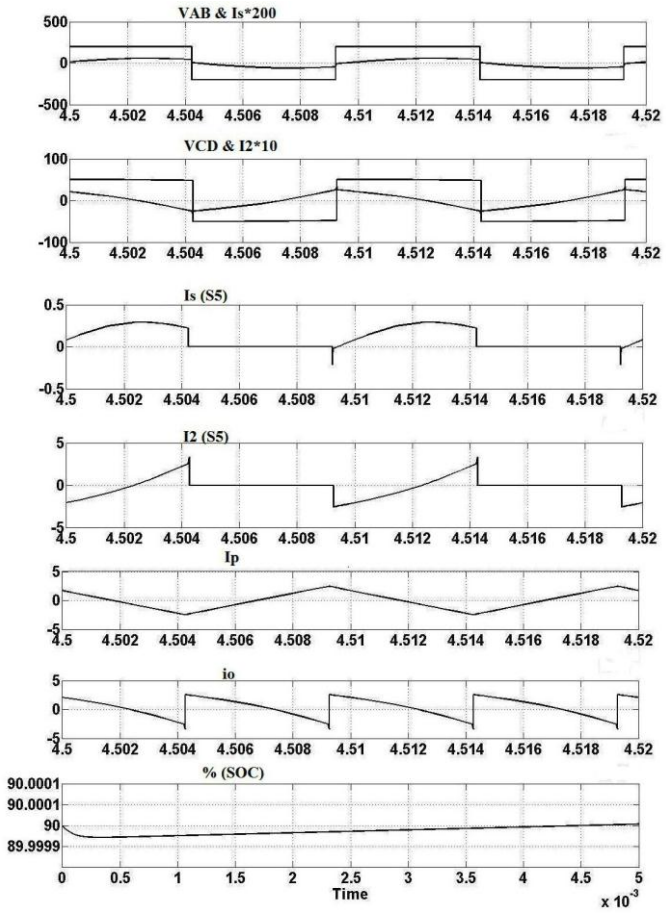

Fig. 7. Simulation Result of LC-L Resonant converter for battery load without PI controller at 90% SOC

C. Digital Control Scheme to Prevent the Reverse Power Flow

Here PI controller is used to prevent the reverse power flow. The combination of proportional and integral terms is important to increase the speed of the response and also to eliminate the steady state error. Fig.8 shows the closed loop control strategy to minimize the reverse power flow. Here the output current (I_o) of converter is compared with the reference value and the error signal is given to PI controller with some gain in error signal. The PI controller process the error signal and produce control signal which given to switch control block. The pulse frequency modulation block generates the frequency pulse according to control signal which maintain unidirectional power flow.

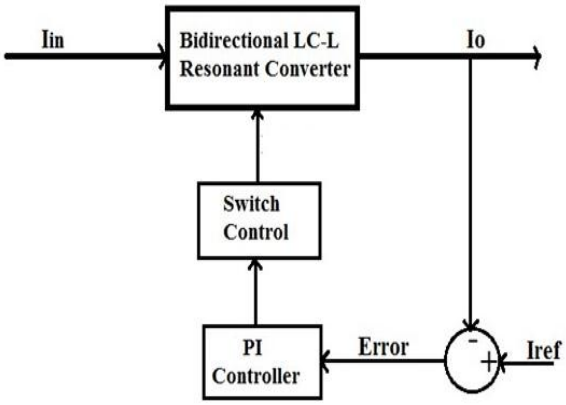

Fig. 8. Closed-loop PI controller diagram for high frequency LC-L resonant converter

The control action of a proportional plus integral controller is defined by following equation:

$$u(t) = K_p\, e(t) + K_i \int e(t)\, dt \qquad (36)$$

Where: *u(t)*- is actuating signal and
e(t) -is error signal.
K_p- Proportional gain constant
K_i - Integral gain constant.

The simulation results with battery load at 90% SOC using PI controller is shown in fig. 9.
The converter works at following conditions:

V_1=200V; V_2=50V; Battery=1.52Ah. 48V, M=0.992, $\emptyset = 1.5^o$, *K_p=1.9, K_i= 0.9.*

From fig. 9, it is observed that by using PI controller the reverse power flowing through converter decreases to large extent and thus it minimizes the losses and increases the efficiency of a converter.

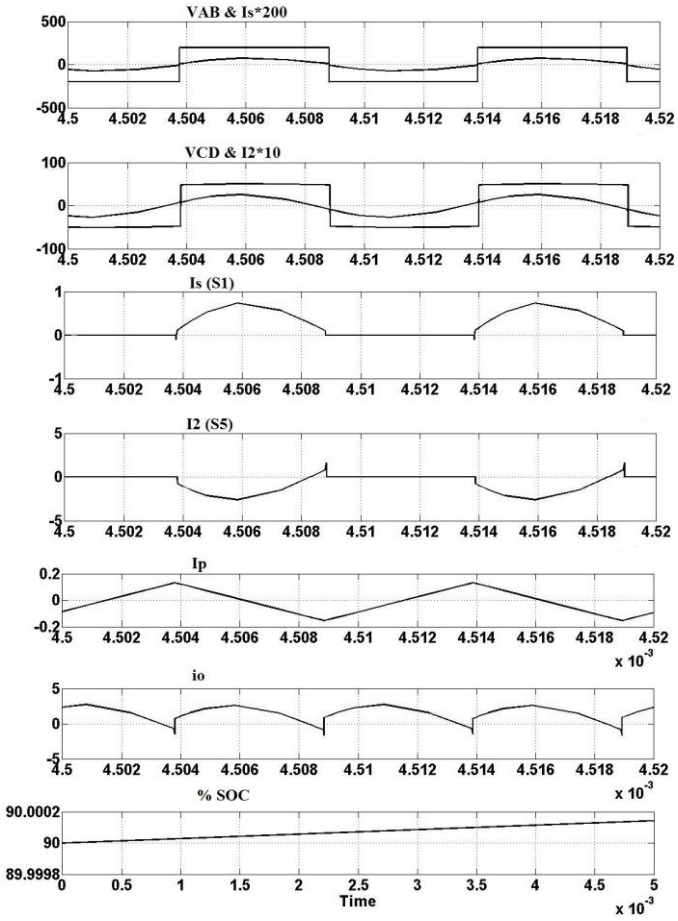

Fig. 9. Simulation results of LC-L resonant converter for battery load with PI controller at 90% SOC

IV. CONCLUSION

In this paper the analysis of dual bridge high frequency series parallel LC-L resonant converter is carried out with modified complex ac analysis approach and accordingly conditions for ZVS are derived for both the bridges. The simulation carried out in Simulink gives the detail view of all operational parameters. The simulation plot validates the theoretical analysis. From simulation it is observed that the ZVS is carried out in both converters. Closed -loop control operation using PI controller is addressed for battery load which increases the converter efficiency by minimizing reverse power flow.

REFERENCES

[1] Huang-Jen Chiu and Li-Wei Lin. "A bidirectional DC-DC converter for fuel cell electric vehicle driving system," *IEEE Transactions on Power Electronics*, vol. 21, no. 4, pages: 950-958, 2006.

[2] Dehong Xu, Chuanhong Zhao, and Haifeng Fan,"A PWM plus phase shift control bidirectional DC-DC

converter," *IEEE Transactions on Power Electronics*, vol. 19, no. 3, pages: 666-675, 2004.

[3] R. W. De Doncker, D. M. Divan and M. H. Kheraluwala, "A three- Phase soft-Switched high power density DC/DC converter for high power applications," *IEEE Trans. Ind. Applicat.*, vol. 27, no. 1, pp. 63-73, Jan./Feb. 1991.

[4] Xiaolong Shi, Jiuchun Jiang and Xintao Guo, "An Efficiency-Optimized Isolated Bidirectional DC-DC Converter with Extended Power Range for Energy Storage Systemsin Microgrids," *Energies* 2013, *6*, 27-44; doi:10.3390/en6010027.

[5] X. D. Li and A. K. S. Bhat, "Analysis and Design of High-Frequency Isolated Dual-Bridge Series Resonant dc/dc Converter," *IEEE Trans. Power Electron.*, vol. 21, no. 2, pp. 850-862, April 2010.

[6] Issa Batarseh, "Resonant converter topologies with three and four energy storage elements," *IEEE Trans. Power Electron.*, vol. 9, no.1, pp. 64-73, Jan. 1994.

[7] X. D. Li and Akshay Rathore, "A general study of soft Switching ranges of dual-bridge resonant converters using a modified complex AC analysis approach," *the 6th IEEE Conference on Industrial Electronics and Applications (ICIEA),* pp: 316-321, June 21-23, Beijing, 2011.

[8] Ashoka K. S. Bhat, "Analysis and Design of LCL-Type Series Resonant Converter," *IEEE Transactions on Industrial electronics*, Vol. 41, No. 1, February 1994.

[9] Kojori H. A., Lavers J. D., and Dewan S. B., "Steady state analysis and design of an inductor-transformer resonant DC-DC converter," *IEEE Industry Appl. Soc. Conf. Rei.*, 1987, pp. 984-989.

[10] Xiaodong Li, Hong-Yu Li, Gao-Yuan Hu and Yu Xue, "A Bidirectional Dual – Bridge High - Frequency Isolated Resonant DC/DC Converter," *Industrial Electronics and Applications (ICIEA), 8th IEEE Conference.* pp. 49 – 54, 19-21, June 2013.